On the dispersed phase boundary conditions in gas-solid flows with irregular particle bouncing

Mohammed Khalij, Arthur Brice Konan-Waidhet, Olivier Simonin, Oesterlé Benoit

On the dispersed phase boundary conditions in gas-solid flows with irregular particle bouncing

M. Khalij[1], A. Konan[2], O. Simonin[2] & B.Oesterlé[1]

[1] LEMTA - UMR 7563 CNRS, ESSTIN, Université Henri Poincaré-Nancy 1,
Rue Jean Lamour, F-54519 Vandoeuvre-lès-Nancy - France
khalij@esstin.uhp-nancy.fr, oesterle@esstin.uhp-nancy.fr
[2] Institut de Mécanique des Fluides de Toulouse, UMR CNRS/INPT/UPS, France
konan@imft.fr, simonin@imft.fr

1 Introduction

The nature of particle-wall collisions is known to play a significant role in confined gas-solid turbulent flows. Besides the possible frictional and/or non elastic character of collisions, the effect of wall roughness is particularly important as it leads to irregular particle bouncing and significant momentum redistribution in the wall normal direction. When using a Lagrangian approach, the collisions against a rough wall can be handled quite easily by means of the so-called "virtual wall" model of Sommerfeld (1992). In two-fluid models however, the particle-wall interactions need to be described by a set of boundary conditions expressing the second and third-order moments of the particle velocities in order to close the transport equations. In the case of a smooth wall, exact boundary conditions have been derived by Sakiz and Simonin (1999) in terms of the restitution coefficient e_w and friction coefficient μ_w. Under the assumption of weak roughness and negligible shadow effect, approximate relationships have been proposed by Simonin et al. (2004) in order to take the wall roughness into account.

The objectives of the present work are :

- to present the derivation of rough wall boundary conditions based on the virtual wall model and to make further proposals aimed at improving the initial theoretical model of Simonin et al. (2004), in order to get expressions of the particle velocity moments at the wall which can be used in the frame of Eulerian-Eulerian approaches ;
- to examine the results of simple numerical simulations performed by computing the reflected velocities of a large number of impacting particles with randomly selected incident velocities, using the virtual wall model ;
- to discuss the obtained statistics by comparison with the approximate expressions of Simonin et al. (2004) and with the improved model proposed herein.

2 Model description

2.1 Rough wall boundary condition derivation

Let us consider the probability distribution function f_p characterizing the statistical properties of the particles. By definition, $f_p(\mathbf{c}_p, \mathbf{x})d\mathbf{c}_p$ is the average number density of particles with velocity $\mathbf{u}_p = \mathbf{c}_p$ in the range of $d\mathbf{c}_p$ measured in an elementary volume around $\mathbf{x}$. Considering any regular function $\mathbf{\Psi}(\mathbf{c}_p)$ of the particle velocity, the mean value of $\mathbf{\Psi}$ writes :

$$\langle \mathbf{\Psi} \rangle_p = \frac{1}{n_p} \int_{R^3} \mathbf{\Psi}(\mathbf{c}_p) f_p(\mathbf{c}_p) d\mathbf{c}_p \qquad \text{with} \qquad n_p = \int_{R^3} f_p(\mathbf{c}_p) d\mathbf{c}_p \tag{1}$$

This equation is used for the definition of the velocity moments (number density, mean velocity, kinetic stresses) computed in the frame of the Eulerian approach.

In order to focus on the effect of the rebound at the wall, we will distinguish the incident and reflected distribution functions when approaching the wall, f_p^+ and f_p^- , restrictions of f_p respectively on $D^+ = \{\mathbf{c}_p \in R^3 \,/\mathbf{c}_p\cdot\mathbf{n} \geq 0\}$ and $D^- = \{\mathbf{c}_p \in R^3 \,/\mathbf{c}_p\cdot\mathbf{n} \leq 0\}$, where $\mathbf{n}$ is the unit vector defined in the wall-normal direction towards the flow. Formally, we can write,

$$f_p^+(\mathbf{c}_p) = f_p(\mathbf{c}_p)H(\mathbf{c}_p\cdot\mathbf{n}) \tag{2}$$

where $H(x)$ is the Heaviside distribution function,

$$H(x) = \begin{cases} 1 & \text{if} \quad x \geq 0 \\ 0 & \text{if} \quad x < 0 \end{cases} \tag{3}$$

The average on incident particles $\langle\cdot\rangle_p^-$ is defined as

$$\langle\mathbf{\Psi}\rangle_p^- = \frac{1}{n_p^-}\int_{R^3} \mathbf{\Psi}(\mathbf{c}_p)f_p^-(\mathbf{c}_p)d\mathbf{c}_p = \frac{1}{n_p^-}\int_{D^-} \mathbf{\Psi}(\mathbf{c}_p)f_p(\mathbf{c}_p)d\mathbf{c}_p \quad \text{with} \quad n_p^- = \int_{R^3} f_p^-(\mathbf{c}_p)d\mathbf{c}_p \tag{4}$$

Similarly, an average on reflected particles $\langle\cdot\rangle_p^+$ can be defined. They are linked by

$$n_p\langle\mathbf{\Psi}\rangle_p = n_p^-\langle\mathbf{\Psi}\rangle_p^- + n_p^+\langle\mathbf{\Psi}\rangle_p^+ \tag{5}$$

We also introduce the transition probability $R(\mathbf{c}_p^- \rightarrow \mathbf{c}_p^+)d\mathbf{c}_p^+$ of an incident particle with velocity $\mathbf{u}_p^- = \mathbf{c}_p^-$ $(\mathbf{c}_p^-\cdot\mathbf{n} < 0)$ to be reflected with a velocity $\mathbf{u}_p^+ = \mathbf{c}_p^+$ in the range of $d\mathbf{c}_p^+$.

If the wall is "particleproof" the velocity of any reflected particle verifies $\mathbf{u}_p^+\cdot\mathbf{n} \geq 0$ (or $\mathbf{u}_p^+ \in D^+$) and this leads to the following normalization condition for the transition probability,

$$\int_{D^+} R(\mathbf{c}_p^- \rightarrow \mathbf{c}_p^+)d\mathbf{c}_p^+ = 1 \ , \tag{6}$$

noticing that the condition above is still valid if the wall-particle interaction model allows particle deposition or rebounds parallel to the wall $(\mathbf{u}_p^+\cdot\mathbf{n} = 0)$.

By assuming no resuspension of particles, meaning that all the particles leaving the wall, $\mathbf{u}_p^+\cdot\mathbf{n} > 0$, are reflected particles, the incident and reflected particle mass fluxes must be equal, yielding the following relation between f_p^+ and f_p^- (cf. Cercignani 1975) :

$$f_p^+(\mathbf{c}_p^+)\,\mathbf{c}_p^+\cdot\mathbf{n} = -\int_{D^-} R(\mathbf{c}_p^- \rightarrow \mathbf{c}_p^+)f_p^-(\mathbf{c}_p^-)\,\mathbf{c}_p^-\cdot\mathbf{n}\,d\mathbf{c}_p^- \qquad \forall\ \mathbf{c}_p^+ \in R^3/\ \mathbf{c}_p^+\cdot\mathbf{n} > 0 \tag{7}$$

If the wall-particle interaction model does not allow particle deposition or rebounds parallel to the wall,

$$R(\mathbf{c}_p^- \rightarrow \mathbf{c}_p^0) = 0 \qquad \forall\ \mathbf{c}_p^0 \in R^3/\ \mathbf{c}_p^0\cdot\mathbf{n} = 0 \tag{8}$$

and the above relation linking f_p^+ and f_p^- is satisfied $\forall\ \mathbf{c}_p^+ \in D^+$.

In the simple case of smooth wall, the reflected velocity of a bouncing particle depends on the incident velocity in a deterministic manner, by means of a rebound law,

$$R(\mathbf{c}_p^- \rightarrow \mathbf{c}_p^+) = \delta\left(\mathbf{c}_p^+ - \mathbf{\Phi}[\mathbf{c}_p^-]\right) \tag{9}$$

Following Sakiz and Simonin (1999), if we make the further assumption that the bouncing is linear in the wall-normal direction, i.e. $\mathbf{\Phi}[\mathbf{c}_p^-]\cdot\mathbf{n} = -e_w\mathbf{c}_p^-\cdot\mathbf{n}$, then equation (7) leads to a direct relation between f_p^+ and f_p^- :

$$f_p^+(\mathbf{c}_p^+) = \frac{1}{e_w J_\Phi} f_p^-\left(\mathbf{\Phi}^{-1}[\mathbf{c}_p^+]\right) \tag{10}$$

where J_Φ is the Jacobian of $\mathbf{\Phi}$. Given this result, a simple relation between the global averages $\langle\cdot\rangle_p$ and the averages on incident particles $\langle\cdot\rangle_p^-$ can be obtained. This relation is used to derive Dirichlet conditions for the particle velocity moments at the wall that have an odd dependence on the wall normal velocity component. But these conditions can also be seen as flux conditions for the moment with an even dependence on the wall normal velocity. For example, in the particle kinetic stress transport model approach (see for example Février and Simonin 1999) Dirichlet conditions are needed for the kinetic shear stress and for the triple velocity correlations which represent the wall-normal fluxes of the mean velocity and kinetic stresses, respectively.

Following Sommerfeld (1992), the transition probability can be linked to the smooth wall bouncing model by introducing a virtual surface with a random angle γ (see Fig. 1) so that

$$R(\mathbf{c}_p^- \rightarrow \mathbf{c}_p^+) = \int_{-\pi/2}^{\pi/2} R_\gamma(\mathbf{c}_p^- \rightarrow \mathbf{c}_p^+) P_r(\gamma|\mathbf{c}_p^-) d\gamma \tag{11}$$

where $P_r(\gamma|\mathbf{c}_p^-)$ is the probability distribution of the virtual wall angle knowing the velocity of the incident particle, by definition,

$$\int_{-\pi/2}^{\pi/2} P_r(\gamma|\mathbf{c}_p^-) d\gamma = 1 \qquad \forall \mathbf{c}_p^- \in D^- \ , \tag{12}$$

and $R_\gamma(\mathbf{c}_p^- \rightarrow \mathbf{c}_p^+)$ is the transition probability on the virtual smooth wall,

$$R_\gamma(\mathbf{c}_p^- \rightarrow \mathbf{c}_p^+) = \delta\left(\mathbf{c}_p^+ - \mathbf{\Phi}_\gamma[\mathbf{c}_p^-]\right) \tag{13}$$

For example, considering only sliding collisions,

$$\mathbf{\Phi}_\gamma[\mathbf{c}_p^-] = \mathbf{c}_p^- - \mathbf{c}_p^- \cdot \mathbf{n}_\gamma (1 + e_w)(\mathbf{n}_\gamma - \mu_w \mathbf{t}_\gamma), \qquad \mathbf{t}_\gamma = \mathbf{v}_\gamma / |\mathbf{v}_\gamma|, \qquad \mathbf{v}_\gamma = \mathbf{c}_p^- - (\mathbf{c}_p^- \cdot \mathbf{n}_\gamma)\mathbf{n}_\gamma \tag{14}$$

with $\mathbf{n}_\gamma = (-\sin\gamma, \cos\gamma, 0)$, and, for elastic bouncing without dynamic friction ($e_w = 1,\ \mu_w = 0$),

$$\mathbf{\Phi}_\gamma[\mathbf{c}_p^-] = \mathbf{c}_p^- - 2(\mathbf{c}_p^- \cdot \mathbf{n}_\gamma)\mathbf{n}_\gamma \tag{15}$$

According to Sommerfeld (1992), the probability distribution of the virtual wall angle is conditioned by the velocity of the incident particles through the so-called "shadow effect". It can be modelled as

$$P_r(\gamma|\mathbf{c}_p^-) = \lambda(\mathbf{c}_p^-) H(-\mathbf{c}_p^- \cdot \mathbf{n}_\gamma) \left(1 - H(-\mathbf{\Phi}_\gamma[\mathbf{c}_p^-] \cdot \mathbf{n})\right) P_r(\gamma) \tag{16}$$

where $H(-\mathbf{c}_p^- \cdot \mathbf{n}_\gamma)$ insures that the particle remains "incident" in the frame of the virtual wall ($\mathbf{c}_p^- \cdot \mathbf{n}_\gamma < 0$) while $\left(1 - H(-\mathbf{\Phi}_\gamma[\mathbf{c}_p^-] \cdot \mathbf{n})\right)$ insures that the reflected particle on the virtual wall will go back towards the flow ($\mathbf{c}_p^+ \cdot \mathbf{n} > 0$).

$P_r(\gamma)$ is the unconditioned probability distribution of the virtual wall angle which may be assumed to be Gaussian :

$$P_r(\gamma) = \frac{1}{\sqrt{2\pi}\,\sigma_\gamma} \exp\left(-\frac{\gamma^2}{2\sigma_\gamma^2}\right), \qquad \sigma_\gamma^2 = \int_{-\pi/2}^{\pi/2} \gamma^2 P_r(\gamma) d\gamma \qquad (\sigma_\gamma \ll \pi/2) \tag{17}$$

and $\lambda(\mathbf{c}_p^-)$ is a parameter which is obtained from the normalization condition (12) :

$$\lambda(\mathbf{c}_p^-) = \left[\int_{-\pi/2}^{\pi/2} H(-\mathbf{c}_p^- \cdot \mathbf{n}_\gamma) \left(1 - H(-\mathbf{\Phi}_\gamma[\mathbf{c}_p^-] \cdot \mathbf{n})\right) P_r(\gamma) d\gamma \right]^{-1} \tag{18}$$

2.2 Particle velocity correlations

Using Eqn. (7), it is possible to write the reflected flux of any function $\psi_p(\mathbf{c}_p)$ in terms of the incident particle velocity distribution,

$$n_p^+ \langle \psi_p u_{p,y} \rangle_p^+ = \int_{D^+} \psi_p(\mathbf{c}_p^+) f_p^+(\mathbf{c}_p^+)\, \mathbf{c}_p^+ \cdot \mathbf{n}\, d\mathbf{c}_p^+ = -\int_{D^+}\int_{D^-} \psi_p(\mathbf{c}_p^+) R(\mathbf{c}_p^- \rightarrow \mathbf{c}_p^+) f_p^-(\mathbf{c}_p^-)\, \mathbf{c}_p^- \cdot \mathbf{n}\, d\mathbf{c}_p^- d\mathbf{c}_p^+ \,, \tag{19}$$

or, introducing the statistical form of the rough wall collision model (11),

$$n_p^+ \langle \psi_p u_{p,y} \rangle_p^+ = -\int_{D^+}\int_{D^-}\int_{-\pi/2}^{\pi/2} \psi_p(\mathbf{c}_p^+) R_\gamma(\mathbf{c}_p^- \rightarrow \mathbf{c}_p^+) P_r(\gamma|\mathbf{c}_p^-) f_p^-(\mathbf{c}_p^-)\, \mathbf{c}_p^- \cdot \mathbf{n}\, d\gamma d\mathbf{c}_p^- d\mathbf{c}_p^+ \tag{20}$$

and the transition probability on the virtual smooth wall (13),

$$n_p^+ \langle \psi_p u_{p,y} \rangle_p^+ = -\int_{D^-}\int_{-\pi/2}^{\pi/2} \psi_p(\mathbf{\Phi}_\gamma[\mathbf{c}_p^-]) P_r(\gamma|\mathbf{c}_p^-) f_p^-(\mathbf{c}_p^-)\, \mathbf{c}_p^- \cdot \mathbf{n}\, d\gamma d\mathbf{c}_p^- \tag{21}$$

In the following, we consider only the case of pure elastic bouncing model, without dynamic friction, but the proposed methodology can be extended directly to more realistic models.

Mass flux ($\psi_p(\mathbf{c}_p) = 1$) **:**

$$n_p^+ \langle u_{p,y} \rangle_p^+ = -\int_{D^-}\int_{-\pi/2}^{\pi/2} P_r(\gamma|\mathbf{c}_p^-) f_p^-(\mathbf{c}_p^-)\, \mathbf{c}_p^- \cdot \mathbf{n}\, d\gamma d\mathbf{c}_p^- = -n_p^- \langle u_{p,y} \rangle_p^- \tag{22}$$

Kinetic shear stress ($\psi_p(\mathbf{c}_p) = c_{p,x}$) **:**

$$\int_{D^+} c_{p,x}^+ f_p^+(\mathbf{c}_p^+)\, \mathbf{c}_p^+ \cdot \mathbf{n}\, d\mathbf{c}_p^+ = -\int_{D^-} \left[\int_{-\pi/2}^{\pi/2} \left(c_{p,x}^- + 2\mathbf{c}_p^- \cdot \mathbf{n}_\gamma \sin\gamma \right) c_{p,y}^- P_r(\gamma|\alpha^-) d\gamma \right] f_p^-(\mathbf{c}_p^-) d\mathbf{c}_p^- \tag{23}$$

or, using a more contracted form,

$$n_p^+ \langle u_{p,x} u_{p,y} \rangle_p^+ = -n_p^- \langle (1 - 2\sin^2\gamma) u_{p,x} u_{p,y} \rangle_p^- - 2n_p^- \langle \sin\gamma \cos\gamma\ u_{p,y} u_{p,y} \rangle_p^- \tag{24}$$

By introducing the mean and fluctuant velocity components,

$$u_{p,x} = U_p + u_p' \,, \qquad u_{p,y} = v_p' \tag{25}$$

the particle kinetic shear stress is written

$$n_p \langle u_p' v_p' \rangle_p = 2n_p^- \langle \sin^2\gamma\ (U_p + u_p') v_p' \rangle_p^- - 2n_p^- \langle \sin\gamma \cos\gamma\ v_p' v_p' \rangle_p^- \tag{26}$$

For practical purpose, we propose to write :

$$n_p \langle u_p' v_p' \rangle_p = 2n_p^- \{\sin^2\gamma\}_p^- \langle (U_p + u_p') v_p' \rangle_p^- - 2n_p^- \{\sin\gamma \cos\gamma\}_p^- \langle v_p' v_p' \rangle_p^- \tag{27}$$

where $\{\cdot\}_p^-$ represents the average weighted by the incident particle number flux,

$$\{\psi_p\}_p^- = \frac{\langle \psi_p u_{p,y} \rangle_p^-}{\langle u_{p,y} \rangle_p^-} \tag{28}$$

For small values of the virtual wall angles ($\sigma_\gamma \ll 1$) Eqn. (27) can be written

$$n_p \langle u'_p v'_p \rangle_p \approx 2 n_p^- \{\gamma^2\}_p^- \langle v'_p \rangle_p^- \, U_p - 2 n_p^- \{\gamma\}_p^- \langle v'_p v'_p \rangle_p^- \tag{29}$$

Finally, the approximate form proposed by Simonin et al. (2004) is obtained by neglecting the "shadow effect" in the modelling of the moments of the virtual wall angle viewed by the incident particles, i.e. $\{\gamma\}_p^- = 0$ and $\{\gamma^2\}_p^- = \sigma_\gamma^2$:

$$n_p \langle u'_p v'_p \rangle_p \approx 2 n_p^- \sigma_\gamma^2 \langle v'_p \rangle_p^- \, U_p \tag{30}$$

Wall normal velocity variance ($\psi_p(\mathbf{c}_p) = c_{p,y}$) :

$$\int_{D^+} c_{p,y}^+ f_p^+(\mathbf{c}_p^+) \, \mathbf{c}_p^+ \cdot \mathbf{n} \, d\mathbf{c}_p^+ = - \int_{D^-} \left[\int_{-\pi/2}^{\pi/2} \left(c_{p,y}^- - 2 \mathbf{c}_p^- \cdot \mathbf{n}_\gamma \cos\gamma \right) c_{p,y}^- P_r(\gamma | \alpha^-) d\gamma \right] f_p^-(\mathbf{c}_p^-) d\mathbf{c}_p^- \tag{31}$$

By introducing the mean and fluctuant velocity components, we obtain

$$n_p \langle v'_p v'_p \rangle_p = 2 n_p^- \langle \cos^2\gamma \; v'_p v'_p \rangle_p^- - 2 n_p^- \langle \sin\gamma \cos\gamma \, (U_p + u'_p) v'_p \rangle_p^- \tag{32}$$

or the approximate form,

$$n_p \langle v'_p v'_p \rangle_p = 2 n_p^- \{\cos^2\gamma\}_p^- \langle v'_p v'_p \rangle_p^- - 2 n_p^- \{\sin\gamma \cos\gamma\}_p^- \langle (U_p + u'_p) v'_p \rangle_p^- \, , \tag{33}$$

and for small values of the virtual wall angles :

$$n_p \langle v'_p v'_p \rangle_p \approx 2 n_p^- \left(1 - \{\gamma^2\}_p^- \right) \langle v'_p v'_p \rangle_p^- - 2 n_p^- \{\gamma\}_p^- \langle (U_p + u'_p) v'_p \rangle_p^- \tag{34}$$

2.3 Discussion and further proposal

Following the approach proposed by Sakiz and Simonin (1999), Eqn. (33) or (34) is used to write the wall-normal velocity variance of incident particles, $\langle v'_p v'_p \rangle_p^-$, in terms of the one predicted in the kinetic stress transport model approach $\langle v'_p v'_p \rangle_p$. And, assuming a half-Gaussian distribution for the incident particle velocities, it is also possible to write the mean incident wall-normal velocity in terms of the incident variance :

$$\langle v'_p \rangle_p^- = - \sqrt{\frac{2}{\pi} \langle v'_p v'_p \rangle_p^-} \tag{35}$$

Finally, the closure of the model approach for the particle kinetic stress wall boundary conditions should be achieved by writing the incident number density n_p^- in terms of the predicted one, n_p. Unfortunately, the derivation proposed by Sakiz and Simonin (1999) for smooth wall cannot be directly extended to rough wall when using the modelling approach proposed by Sommerfeld (1992). Indeed, we found that, when using the probability distribution of the virtual wall angle modified by the "shadow effect" given by Eqn. (16) and assuming a half-Gaussian incident velocity distribution, the ratio n_p^+ / n_p^- is not limited ($n_p^+ / n_p^- \to \infty$). This effect is due to the fact that the virtual wall angle probability distribution given by (16) leads to "large" values of the transition probability (11) for particle with non-zero incident wall-normal velocity ($\mathbf{u}_p^- \cdot \mathbf{n} \approx - \langle v'_p \rangle_p^-$) to bounce with nearly zero reflecting velocity $\mathbf{u}_p^+ \cdot \mathbf{n} \approx 0$. So, after bouncing, these particles will have flat trajectories parallel to the wall and contribute to the divergence of the reflected to incident particle number density ratio. This spurious effect

could be avoided by two separate ways, by modifying the probability distribution of the virtual angle for very small values of the reflected angle with respect to the wall, or by modifying the presumed shape of the incident velocity distribution to account for the interactions with the grazing particles.

Based on the numerical simulation results presented hereafter, we have proposed another approach based on an additional closure assumption for the reflected velocity distribution. Indeed, we have assumed that the mean incident wall-normal velocity can be written in terms of the reflected variance :

$$\langle v_p' \rangle_p^+ = \lambda^+ \sqrt{\langle v_p' v_p' \rangle_p^+} \tag{36}$$

This parameter λ^+ should be equal to $\lambda^- = -\langle v_p' \rangle_p^- / \sqrt{\langle v_p' v_p' \rangle_p^-}$ if the reflected velocity probability distribution is also Gaussian, but we shall see from the simulation results that λ^+ is found to be equal to about $0.4\lambda^-$. Nevertheless, so far we have no physical explanation of such a value.

3 Numerical simulations based on the velocity PDF of impacting particles

3.1 Simulation principle

For each specification of the collision parameters e_w, μ_w and σ_γ (standard deviation of the virtual wall inclination), a large number of particle rebounds (from 10^7 to $5 \cdot 10^8$) are simulated. The wall roughness is taken into account by means of the two-dimensional virtual wall model (Sommerfeld 1992) described in § 2.1. The virtual wall is obtained by rotating the actual wall around the z-axis which is perpendicular to both the incident velocity vector and the wall normal vector, as shown by Fig. 1.

The particle velocity components in the fixed reference frame are denoted u_p, v_p, w_p, the mean particle velocity $U_p = \langle u_p \rangle$ is in the x-direction and y denotes the wall normal direction. We restrict ourselves to the case $w_p = 0$, so that the translational and rotational velocity components are fully disconnected (Sakiz and Simonin 1999). For each simulated particle, the incident velocity components u_p^- and v_p^- are randomly and independently selected according to the following rules :

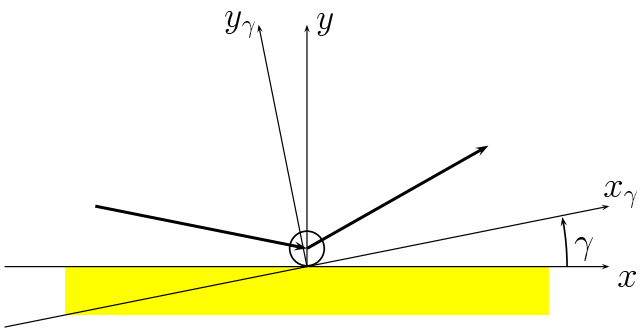

Figure 1: Co-ordinate system and definition of the virtual wall inclination γ.

- the tangential incident particle velocity is assumed to obey a Gaussian distribution with given standard deviation σ_u^- and mean value $\langle u_p \rangle_p^-$.

- the wall normal incident velocity obeys a given statistical distribution restricted to negative values (see Fig. 1), obtained in assuming a semi-Gaussian velocity PDF at the wall

with prescribed standard deviation $\sigma_v^- = \sqrt{\langle v_p' v_p' \rangle_p^-}$, i.e.

$$f_{p,y}^-(c_{p,y}) = \frac{2\, n_p^-}{\sigma_v^- \sqrt{2\pi}} \exp(-\frac{c_{p,y}^2}{2(\sigma_v^-)^2})$$

for $c_{p,y} \leq 0$. As the number of particles impacting the wall with velocity $c_{p,y}$ during time dt is proportional to $|c_{p,y}| f_{p,y}^-(c_{p,y}) dt$, the wall normal velocity of the incident particles obeys the following distribution function $f_{inc}(c_{p,y})$, normalized such as $\int_{-\infty}^{0} f_{inc}(c_{p,y}) dc_{p,y} = 1$:

$$f_{inc}(c_{p,y}) = -\frac{c_{p,y}}{(\sigma_v^-)^2} \exp\left(-\frac{c_{p,y}^2}{2(\sigma_v^-)^2}\right) \tag{37}$$

As $f_{inc}(c_{p,y})$ can be analytically integrated to obtain the corresponding cumulative distribution function $F_{inc}(c_{p,y}) = \int_{-\infty}^{c_{p,y}} f_{inc}(v) dv = \exp(-c_{p,y}^2/(2(\sigma_v^-)^2))$, the process of random generation of the wall normal incident particle velocity consists in selecting a uniformly distributed random variable $Z \in [0,1]$, and writing $v_p^- = F_{inc}^{-1}(Z)$, i.e. :

$$v_p^- = -\sqrt{-2(\sigma_v^-)^2 \ln Z} \tag{38}$$

The distribution of the virtual wall inclination angle is taken as Gaussian with given standard deviation σ_γ and zero mean value. A new angle γ is generated for each particle. In order to take the shadow effect into consideration according to Eqn. (16), any unphysical rebound is disregarded, i.e. the incident particle velocity must be directed towards the virtual wall, and the reflected velocity must be directed outwards the actual wall. As a consequence, the actual distribution of γ is modified and the actual mean value $\{\gamma\}_p^-$ will be positive. The prescribed standard deviation σ_γ is varied from 0 to 0.2 according to the results of Sommerfeld and Huber (1999), who showed that the optimum value of σ_γ decreases with increasing particle diameter for a given physical roughness.

For each particle, the postcollisional velocity components are determined from the standard rebound law (14) assuming sliding collisions.

3.1.1 Computation of the particle statistical moments

The mean value of any quantity ψ_p is written according to Eqn. (5). As already mentioned, the simulated particle flux is proportional to $|v_p|$, therefore the averages based on the particle velocity distribution function at the wall are to be computed following Sakiz and Simonin (1999), i.e.

$$\langle \psi_p \rangle_p^- = \frac{\{\psi_p / v_p\}_p^-}{\{1/v_p\}_p^-}\ , \quad \langle \psi \rangle_p^+ = \frac{\{\psi_p / v_p\}_p^+}{\{1/v_p\}_p^+} \tag{39}$$

where the flux average $\{\cdot\}_p$, defined by Eqn. (28), is merely the arithmetic mean operated on the impacting particles, $\{\cdot\}_p = \frac{1}{N}\sum_1^N$, N being the number of simulated collisions.

As in a real flow without deposition the particle mass flux at the wall must be zero, the weighting factors entering the mean value expression (5) are determined from Eqn. (22) which leads to :

$$\frac{n_p^-}{n_p} = \frac{\langle v_p \rangle_p^+}{\langle v_p \rangle_p^+ - \langle v_p \rangle_p^-}\ , \quad \frac{n_p^+}{n_p} = -\frac{\langle v_p \rangle_p^-}{\langle v_p \rangle_p^+ - \langle v_p \rangle_p^-} \tag{40}$$

where $\langle v_p \rangle_p^- = \left(\{1/v_p\}_p^-\right)^{-1}$ and $\langle v_p \rangle_p^+ = \left(\{1/v_p\}_p^+\right)^{-1}$.

3.1.2 Comparison with the exact expressions in case of smooth wall

Before performing the simulation in the rough wall case, comparison was carried out with the exact expressions of the second and third-order particle velocity moments derived by Sakiz and Simonin (1999) for a smooth wall. These expressions are valid under the assumption of sliding collisions and negligible velocity in the spanwise direction. The moments involving the fluctuating velocity components u'_p and v'_p are :

$$\langle u'_p v'_p \rangle_p = -\mu_w e_w \langle v'_p v'_p \rangle_p^- \quad (41)$$

$$\langle v'_p v'_p \rangle_p = e_w \langle v'_p v'_p \rangle_p^- \quad (42)$$

$$\langle u'_p u'_p v'_p \rangle_p = -2\mu_w \langle u'_p v'_p v'_p \rangle_p - \mu_w^2 e_w (1 - e_w) \langle v'_p v'_p v'_p \rangle_p^- \quad (43)$$

$$\langle u'_p v'_p v'_p \rangle_p = e_w \langle u'_p v'_p v'_p \rangle_p^- + \mu_w e_w^2 \langle v'_p v'_p v'_p \rangle_p^- \quad (44)$$

For each set of parameters e_w and μ_w, the simulation results were found in perfect agreement with these theoretical expressions.

3.2 Simulation results

As the velocity statistics of the incident particles are prescribed in the simulation, the quantities of particular interest are the velocity average $\langle v_p \rangle_p^+$, which yields the ratio n_p^+/n_p^- or the weighting factors according to Eqn. (40), and the second and third-order moments of the reflected particles. For sake of conciseness, in this part the presentation is restricted to the numerical predictions of n_p^+/n_p^- (or n_p^-/n_p) and of the particle kinetic stresses $\langle u'_p v'_p \rangle_p$ and $\langle v'_p v'_p \rangle_p$.

3.2.1 Effect of roughness in case of perfect collisions ($e_w = 1$, $\mu_w = 0$)

First, we examine the roughness effect in the case of elastic frictionless collisions. The following statistics are prescribed for the incident particles (in arbitrary units) : $\sigma_u^- = 1$, $\sigma_v^- = \sqrt{\langle v'_p v'_p \rangle_p^-} = 1$ (it must be noticed that the prescribed standard deviation σ_u^- is slightly different from $\sqrt{\langle u'_p u'_p \rangle_p^-}$ due to the difference between U_p and $\langle u_p \rangle_p^-$). In order to investigate the effect of varying the average impact angle, several values of the mean velocity of the incident particles are tested, namely $\langle u_p \rangle_p^- = 0$; 1; 2; 5 and 10.

In Fig. 2, the ratio $n_p^+/n_p^- = -\langle v_p \rangle_p^- / \langle v_p \rangle_p^+$ is displayed as a function of σ_γ^2, the prescribed variance of the virtual wall inclination. In connection with the variation of $\langle v_p \rangle_p^+$ which is always significantly lower than $\langle v_p \rangle_p^-$, we observe first an increase in n_p^+/n_p^- followed by a slow decrease with increasing roughness parameter σ_γ^2. However, besides this general trend, the main particularity of the observed statistics lies in the presence of some irregular peaks with very large values of n_p^+/n_p^-, depending of the simulation run (see Fig. 2, left) in spite of the huge number of simulated particle-wall collisions. This behavior confirms the conclusion from the above theoretical model in § 2.3 about the possible occurrence of "grazing" rebounds with very small reflected velocity in the wall normal direction, which may take place for any negative value of γ. As shown by Fig. 2 (right), there is no obvious influence of the mean particle velocity $\langle u_p \rangle_p^-$, except at very small values of σ_γ^2 for which n_p^+/n_p^- can be observed to significantly increase with increasing incident velocity $\langle u_p \rangle_p^-$. Clearly, the results show that there is still a large uncertainty on the ratio n_p^+/n_p^-. The development of some accurate model for this quantity using the present virtual wall model remains therefore an open issue, and this is the reason why the modelling efforts presented in the previous section have been

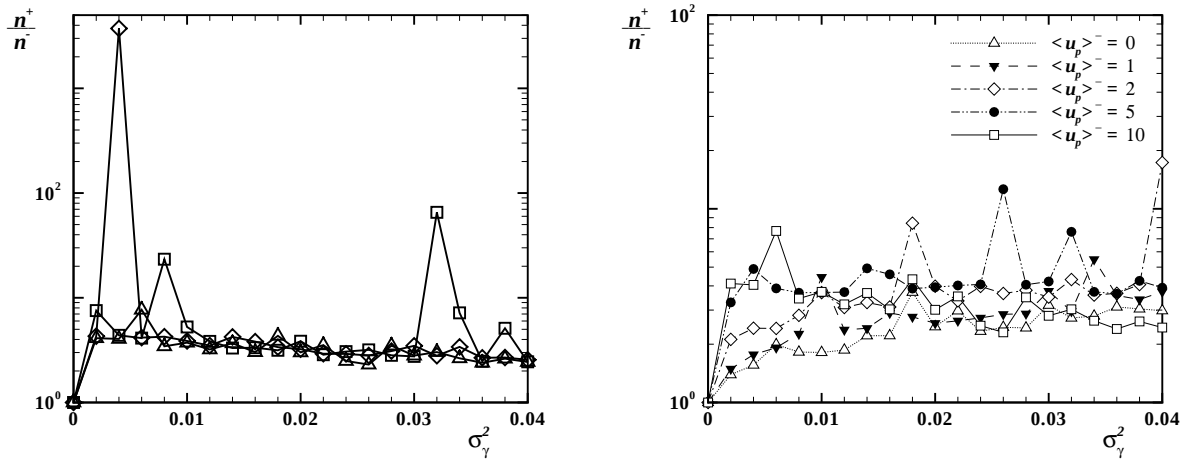

Figure 2: The ratio n_p^+/n_p^- as a function of σ_γ^2. Left : three different simulation runs for $\langle u_p \rangle_p^- = 10$. Right : results for $\langle u_p \rangle_p^- = 0$; 1; 2; 5 and 10.

directed towards the derivation of some approximate relationships between the particle velocity moments before and after collision independently from the ratio n_p^+/n_p^-.

Focusing on the second-order moment $\langle u_p' v_p' \rangle_p$ in this case ($e_w = 1$, $\mu_w = 0$), let us recall that the approximate expression proposed by Simonin et al. (2004) for $\sigma_\gamma \ll 1$ and negligible shadow effect is obtained from Eqn. (30) by setting $n_p^- = n_p/2$:

$$\langle u_p' v_p' \rangle_p \approx \sigma_\gamma^2 \langle v_p' \rangle_p^- \, U_p \tag{45}$$

It can be observed from Fig. 3 (a) that the agreement with Eqn. (45) is qualitatively satisfactory, even if this expression is seen to somewhat overestimate the momentum flux $\langle u_p' v_p' \rangle_p$. Whereas there is no significant effect of the ratio $\langle u_p \rangle_p^- / \langle v_p' \rangle_p^-$ for small roughness parameter, at larger values of σ_γ better agreement is obtained for the highest incident velocity $\langle u_p \rangle_p^-$, which corresponds to lower values of n_p^+/n_p^- according to Fig. 2 (right). Keeping in mind that Eqn. (45) was obtained in assuming $n_p^+ = n_p^-$, it is clear that the explanation of such an overestimation can be found in Fig. 2 where n_p^+/n_p^- was shown to always exceed unity.

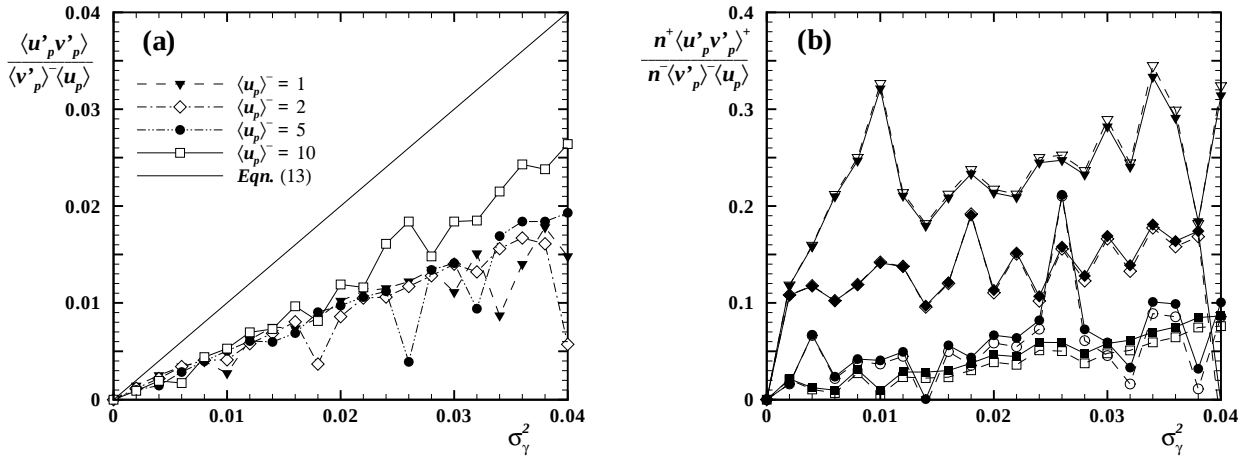

Figure 3: (a) The ratio $\langle u_p' v_p' \rangle_p / (U_p \langle v_p' \rangle^-)$ as a function of σ_γ^2 for several values of $\langle u_p \rangle_p^-$, comparison with Eqn. (45). (b) Comparison between the numerical prediction and Eqn. (47) for $n_p^+ \langle u_p' v_p' \rangle_p^+$; same symbol shapes as (a), filled symbols : numerical simulation, open symbols : Eqn. (47).

Before examining the proposal made in § 2.3 to achieve satisfactory closure for the number density ratio, and therefore for any particle velocity moment at the wall, let us have a look at the approximations made in the derivation of the simplified shear stress expression (30). According to Eqn. (24), the exact expression of $n_p^+ \langle u'_p v'_p \rangle_p^+$ can be written

$$n_p^+ \langle u'_p v'_p \rangle_p^+ = -n_p^- \langle u'_p v'_p \rangle_p^- + 2n_p^- \langle (U_p + u'_p) v'_p \sin^2\gamma \rangle_p^- - 2n_p^- \langle v'_p v'_p \sin\gamma \cos\gamma \rangle_p^- \,, \qquad (46)$$

while Eqn. (30) was obtained by replacing the mean value of some products by the products of the averages, and by using further approximations based on the assumptions $\sigma_\gamma \ll 1$ and negligible shadow effect, leading to :

$$n_p^+ \langle u'_p v'_p \rangle_p^+ \approx -n_p^- \langle u'_p v'_p \rangle_p^- + 2n_p^- \sigma_\gamma^2 \langle v'_p \rangle_p^- \, U_p \qquad (47)$$

It is therefore interesting to examine the validity of the latter approximations. This is the aim of Fig. 3 (b), where our numerical predictions for $n_p^+ \langle u'_p v'_p \rangle_p^+$ are compared with Eqn.(47) put under dimensionless form by dividing by $n_p^- \langle v'_p \rangle_p^- \, U_p$. The approximations leading from (46) to (47) can be seen to provide satisfactory agreement over the range of σ_γ investigated here.

3.2.2 The influence of the restitution and friction coefficients

Following the derivation by Simonin et al. (2004), in case of inelastic and frictional collisions and under the assumption of low virtual wall inclination, the total kinetic stresses can be considered as the sum of the part due to friction and imperfect restitution as for a smooth wall, which obeys Eqn. (41), and the part due to roughness as if the collision were perfect. Considering the example of the momentum flux $\langle u'_p v'_p \rangle$, this decomposition can be written

$$\langle u'_p v'_p \rangle_p = -\mu_w \langle v'_p v'_p \rangle_p + \langle u'_p v'_p \rangle_R \,, \qquad (48)$$

where the contribution due to roughness, denoted here by $\langle u'_p v'_p \rangle_R$, should not significantly depend on the restitution and friction coefficients. This is confirmed by Fig. 4, where the numerically predicted values of $\langle u'_p v'_p \rangle_R$ are displayed for several values of friction and restitution

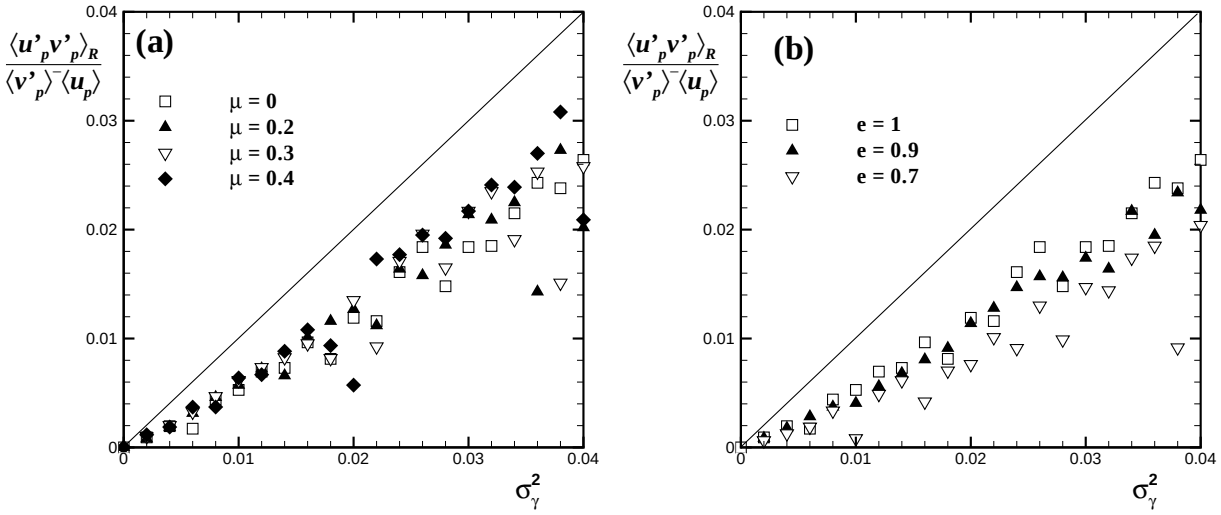

Figure 4: The roughness induced kinetic stress part $\langle u'_p v'_p \rangle_R$ (a) for $e_w = 1$ and several values of the friction coefficient, (b) for $\mu_w = 0.2$ and several values of the restitution coefficient ($\langle u_p \rangle_p^- = 10$ in both plots). Solid line : Eqn. (45).

coefficients. The roughness induced part of $\langle u'_p v'_p \rangle_p$ can be seen to match the predictions shown in Fig. 3 (a), with a slight exception for the smallest value of the restitution coefficient which seems to induce some decrease in $\langle u'_p v'_p \rangle_R$.

3.2.3 Assessment of the closure assumption about the reflected velocity distribution

Following the suggestion $\langle v'_p \rangle_p^+ = -\lambda^+ \sqrt{\langle v'_p v'_p \rangle_p^+}$, we investigate here the possibility of considering λ^+ as a constant model parameter. Using this assumption, it is possible to close the particle velocity moment equations, as explained in § 2.3.

Therefore the ratio λ^+/λ^- was extracted from the simulation results under various sets of parameters, namely $\sigma_u^- / \sqrt{\langle v'_p v'_p \rangle_p^-} = 2$ and $\langle u_p \rangle_p^- / \sqrt{\langle v'_p v'_p \rangle_p^-} = 5$, 10 and 30, for frictionless elastic bouncing. As shown by Fig. 5, the numerical predictions confirm that the ratio λ^+/λ^- is almost constant except for very small σ_γ, and that an acceptable approximation is $\lambda^+/\lambda^- \approx 0.4$.

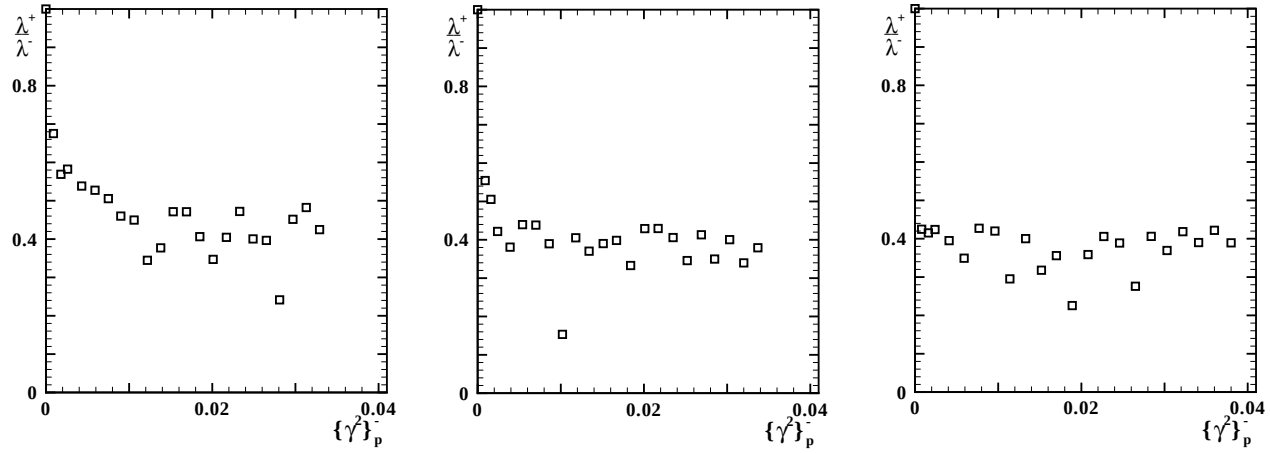

Figure 5: The numerically predicted ratio λ^+/λ^- as a function of $\{\gamma^2\}_p^-$ for $\langle u_p \rangle_p^- / \sqrt{\langle v'_p v'_p \rangle_p^-} = 5$ (left), 10 (middle) and 30 (right).

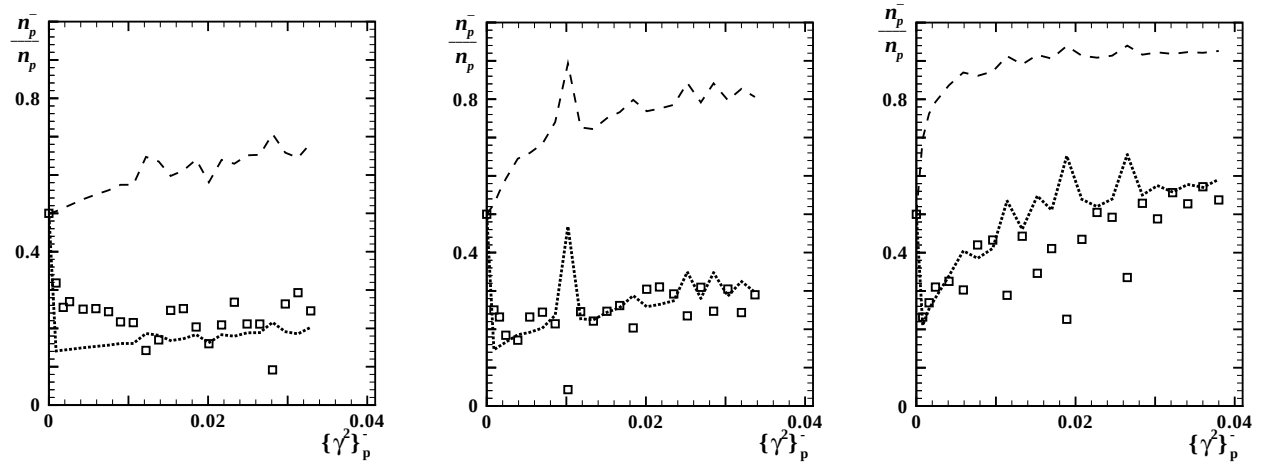

Figure 6: The ratio n_p^-/n_p as a function of $\{\gamma^2\}_p^-$ for $\langle u_p \rangle_p^- / \sqrt{\langle v'_p v'_p \rangle_p^-} = 5$ (left), 10 (middle) and 30 (right). Symbols: numerical; lines: enhanced model with $\lambda^+ = \lambda^-$ (dashed) and $\lambda^+ = 0.4\lambda^-$ (dotted).

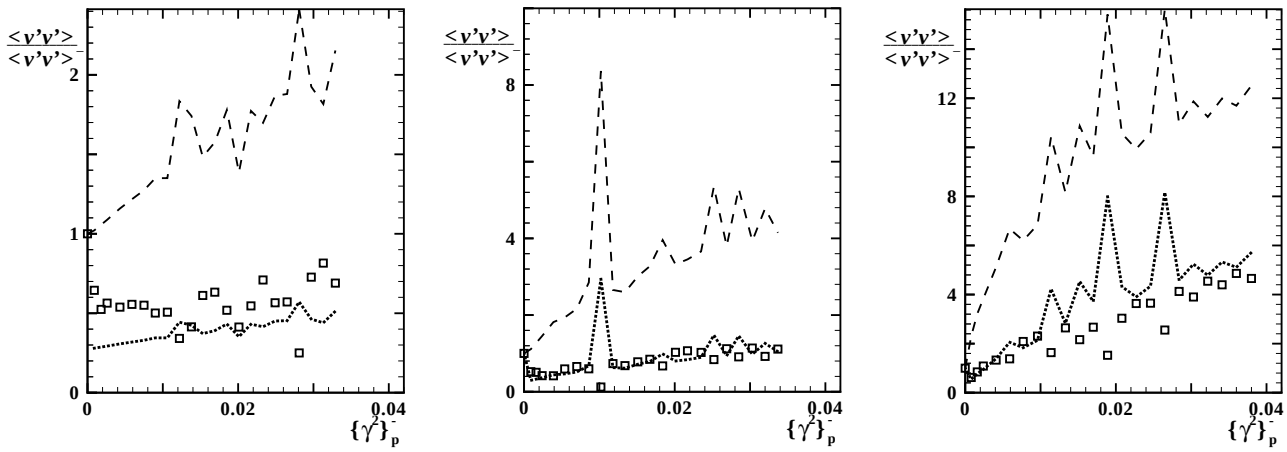

Figure 7: The ratio $\langle v'_p v'_p \rangle_p / \langle v'_p v'_p \rangle_p^-$ as a function of $\{\gamma^2\}_p^-$ for $\langle u_p \rangle_p^- / \sqrt{\langle v'_p v'_p \rangle_p^-} = 5$ (left), 10 (middle) and 30 (right). Symbols: numerical; lines: enhanced model with $\lambda^+ = \lambda^-$ (dashed) and $\lambda^+ = 0.4\lambda^-$ (dotted).

(Note that in Fig. 5, as well as in Figs. 6-8, the results are plotted in terms of the actual variance of the virtual wall inclination, $\{\gamma^2\}_p^-$).

The analytical predictions of n_p^-/n_p, $\langle v'_p v'_p \rangle_p$ and $\langle u'_p v'_p \rangle_p$ obtained using $\lambda^+/\lambda^- = 0.4$ are displayed in Figs. 6-8, where a comparison is provided with the assumption $\lambda^+/\lambda^- = 1$ which would be valid if the reflected velocity PDF were Gaussian. It can be seen that the model predictions with $\lambda^+/\lambda^- = 0.4$ are in very good agreement with the numerical simulation, contrary to what would be obtained with $\lambda^+ = \lambda^-$, an assumption that is observed to lead to the non physical result $n_p^- > n_p/2$. In Fig. 8, the computed and modelled kinetic shear stresses are also compared with the simple expression (45) based on the hypothesis $n_p^- = n_p/2$. Even if the discrepancies between the various models decrease with increasing mean velocity, it clearly appears that the enhanced model with $\lambda^+/\lambda^- = 0.4$ provides very satisfactory predictions of the particle velocity correlations at the wall in the range of roughness parameter investigated here, i.e. $\sigma_\gamma \leq 0.2$.

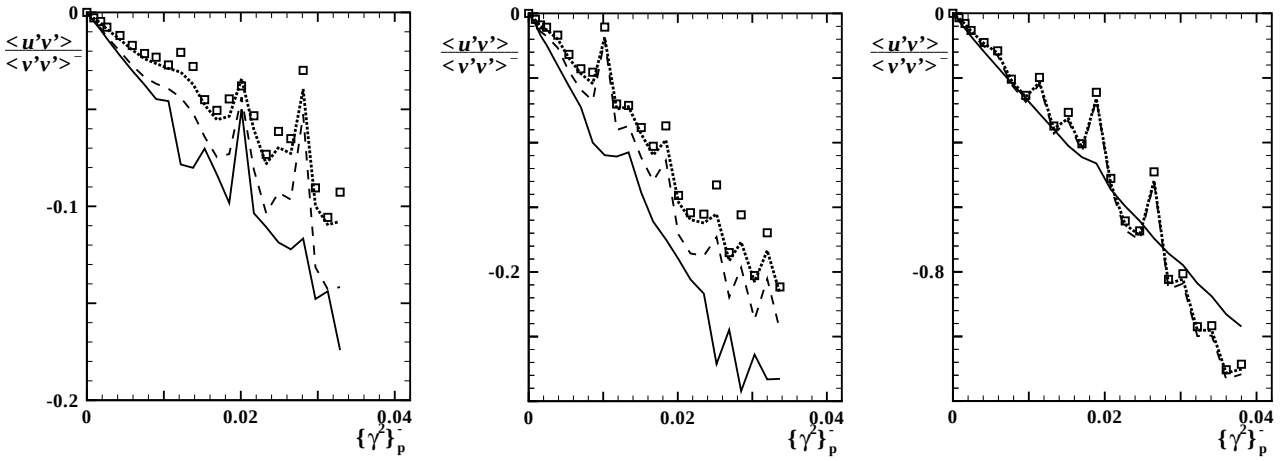

Figure 8: The kinetic shear stress $\langle u'_p v'_p \rangle_p$ as a function of $\{\gamma^2\}_p^-$ for $\langle u_p \rangle_p^- / \sqrt{\langle v'_p v'_p \rangle_p^-} = 5$ (left), 10 (middle) and 30 (right). Symbols: numerical; lines: Eqn. (45) (solid), enhanced model with $\lambda^+ = \lambda^-$ (dashed) and $\lambda^+ = 0.4\lambda^-$ (dotted)

4 Conclusion

An analytical derivation of rough wall boundary conditions based on the virtual wall model and including the so-called shadow effect has been presented. Particular emphasis has been put on the issue of predicting the number density ratio of reflected to incident particles, n_p^+/n_p^-, and a new approach has been suggested in order to get expressions of the particle velocity moments at the wall which can be used in the frame of Eulerian-Eulerian approaches.

The theoretical study has been supplemented by numerical simulations performed by computing the reflected velocities of a large number of impacting particles with randomly selected incident velocities, using the virtual wall model. The obtained statistics, which confirm the possible divergence of the ratio n_p^+/n_p^-, have been first compared with the approximate expression of the kinetic shear stress $\langle u_p' v_p' \rangle_p$ proposed by Simonin et al. (2004) based on the simple assumption $n_p^+/n_p^- = 1$. Even if qualitative agreement is obtained, the comparison shows that better estimation of this ratio is needed to improve the accuracy of the model. Therefore the simulation results have been used to assess the new approach, which is based on an assumption for the reflected velocity distribution. It has been shown that the enhanced model leads to very good agreement with the numerical predictions provided the main parameter in this model, $\lambda^+ = \langle v_p' \rangle_p^+ / \sqrt{\langle v_p' v_p' \rangle_p^+}$, is taken equal to $0.4\lambda^- = -0.4\langle v_p' \rangle_p^- / \sqrt{\langle v_p' v_p' \rangle_p^-}$. As we have no physical explanation for such a result, further investigations have to be carried out in order to examine the link between the probability distributions of incident and reflected particle velocity.

References

Cercignani, C.: 1975, *Theory and application of the Boltzmann equation*, Elsevier, New York.

Février, P. and Simonin, O.: 1999, Development and validation of a fluid and particle turbulent stress transport model in gas-solid flows, *in* M. Sommerfeld (ed.), *Proceedings 9th Workshop on Two-Phase Flow Predictions*, Merseburg, Germany, pp. 77–85.

Sakiz, M. and Simonin, O.: 1999, Development and validation of continuum particle wall boundary conditions using Lagrangian simulation of a vertical gas-solid channel flow, *Proceedings 3rd ASME/JSME Joint Fluids Engng. Conf.*, San Francisco, CA. Paper No 7898.

Simonin, O., Fede, P., Patino, G. and Squires, K.: 2004, Mathematical models and closure laws for gas-particle turbulent flows, *Proceedings of the ICMF'04, 5th Int. Conf. Multiphase Flows*, Yokohama, Japan. Paper No K08.

Sommerfeld, M.: 1992, Modelling of particle-wall collisions in confined gas-particle flows, *Int. J. Multiphase Flow* **18**, 905–926.

Sommerfeld, M. and Huber, N.: 1999, Experimental analysis and modelling of particle-wall collisions, *Int. J. Multiphase Flow* **25**, 1457–1489.